Poljak, R. J., Amzel, L. M., Avey, H. P., Chen, B. L., Phizackerley, R. P., & Saul, F. (1973) *Proc. Natl. Acad. Sci. U.S.A. 70*, 3305–3310.
Ponstingl, H., Hess, M., & Hilschmann, N. (1968) *Hoppe-Seyler's Z. Physiol. Chem. 349*, 867–871.
Putnam, F. W., Titani, K., Wikler, M., & Shinoda, T. (1967) *Cold Spring Harbor Symp. Quant. Biol. 32*, 9–29.
Solomon, A. (1977) *Immunogenetics 5*, 525–533.
Takahashi, N., Takayasu, T., Shinoda, T., Okuyama, N., Ito, S., & Shimizu, A. (1979) *Seikagaku 51*, 716.
Takayasu, T., Takahashi, N., Shinoda, T., Okuyama, N., & Tomioka, H. (1979) *Seikagaku 51*, 812.
Tsuzukida, Y., Wang, C., & Putnam, F. W. (1979) *Proc. Natl. Acad. Sci. U.S.A. 76*, 1104–1108.
Wikler, M., Titani, K., Shinoda, T., & Putnam, F. W. (1967) *J. Biol. Chem. 242*, 1668–1670.

A Common Mechanism of Hapten Binding to Immunoglobulins and Their Heterologous Chain Recombinants†

Raphael Zidovetzki, Yoav Blatt, Cornelis P. J. Glaudemans, Belur N. Manjula, and Israel Pecht*

ABSTRACT: Kinetics and thermodynamics of binding of the hapten β-D-(1–6)-galactotriose to the homogeneous IgA T-601 and to heterologous recombinants of heavy and light chains prepared from mouse myeloma IgA's X-24, J-539, and T-601, which all have the same galactan specificity, have been studied by the chemical relaxation method. All the immunoglobulin–hapten systems investigated were found to exhibit two relaxation times. The reciprocal value of the fast time increased linearly, while that of the slow time leveled off with increasing hapten concentration. This behavior indicates the presence of a fast bimolecular association and a slower monomolecular step. The data obtained for homologous and hybrid immunoglobulins were all found to fit a mechanism where the proteins exist in two conformations and hapten binding shifts their equilibrium to the higher affinity conformer. Furthermore, the kinetic and thermodynamic parameters for the hapten binding by the hybrids were found to be similar to those of their parent proteins. These results strongly suggest that this conformational transition is an inherent property of the tertiary domain structure of the antibody, probably involving changes in the interactions between heavy- and light-chain domains.

X-ray crystallographic studies of several human and murine immunoglobulins (Ig's)[1] and their fragments have shown that the chains of all these molecules are folded into a linear series of compact domains having similar tertiary structure [for reviews, see Poljak et al. (1976) and Padlan (1977)]. Each domain corresponds to one of the homology regions apparent in the primary structures of these chains. Residues involved in making both inter- and intrachain contacts between domains are highly conserved even in the variable regions and are often identical in closely related Ig's (Poljak, 1975). Thus, the mode of association between domains, including the variable ones (V_L and V_H), has been assumed to be the same or at least very similar in all antibody molecules (Padlan, 1977). This assumption has been confirmed by extensive studies where heavy and light chains, separated from their parent Ig's in dissociating solvents, were successfully reassembled to form the characteristic four-chain structure [for references, see Manjula et al. (1976) and Klein et al. (1979)]. When heterologous recombinants were similarly prepared by using heavy and light chains derived from different parent Ig's, the hybrid molecules usually exhibited a substantial reduction in hapten binding affinity and idiotypic activity as compared with those properties in their parent molecules (Manjula et al., 1976). A notable exception is a group of hybrid Ig's prepared by heterologous recombination of heavy and light chains made from the β-D-(1–6)-oligogalactan-specific homologous murine myelomas X-24, J-539, and T-601. The parent proteins are of the IgA class with κ light chains of the same variable region subgroup. The hybrids maintain an affinity for the same haptens which is comparable to that of their parent molecules (Manjula et al., 1976, 1977).

The mechanism of binding of two oligogalactose haptens to two of the above immunoglobulins, X-24 and J-539, has been examined by kinetic measurements using the chemical relaxation–temperature jump method (Vuk-Pavlović et al., 1978). This investigation produced evidence for a hapten binding induced conformational transition in both immunoglobulins. Such a hapten binding linked transition was reported previously for the poly(nitrophenyl)-specific IgA_κ secreted by plasmacytoma MOPC-460 (Lancet & Pecht, 1976).

The question arose as to whether the observed conformational transition is an inherent property of the interacting heavy and light chains. A solution might be found in the behavior of hybrid molecules produced from Ig's which have been already investigated. The present work examines the kinetics and thermodynamics of binding of β-D-(1–6)-galactotriose (Gal_3) to the homologous IgA T-601 and to the hybrid recombinants $H^{24}L^{539}$, $H^{539}L^{24}$, $H^{24}L^{601}$, and $H^{601}L^{24}$. The results show that the heterologous recombinants exhibit the same kinetic pattern of binding as their parent proteins. Thus, the conformational transitions linked to hapten binding appear to

† From the Department of Chemical Immunology, The Weizmann Institute of Science, Rehovot, Israel (R.Z., Y.B., and I.P.), and the National Institute of Arthritis, Metabolism and Digestive Diseases, National Institutes of Health, Bethesda, Maryland 20014 (C.P.J.G. and B.N.M.). *Received December 18, 1979.* The Fritz Thyssen Foundation is gratefully acknowledged for its support of this research.

[1] Abbreviations used: Ig, immunoglobulin; IgA, immunoglobulin A; Fab, antigen binding fragment of Ig; Fd, NH_2-terminal half of a heavy chain; H, heavy chain of Ig; L, light chain of Ig; V, variable region; C, constant region; CDR, complementarity-determining region; FR, framework region; Gal_3, β-D-(1–6)-galactotriose; ESR, electron spin resonance; NMR, nuclear magnetic resonance.

0006-2960/80/0419-2790$01.00/0

be a general property of the antibody molecule, probably implemented as changes in the interactions between heavy- and light-chain domains.

Materials and Methods

Protein T-601 and the hybrids $H^{24}L^{539}$, $H^{539}L^{24}$, $H^{24}L^{601}$, and $H^{601}L^{24}$ of the galactan-binding Ig's were prepared according to the described procedure (Manjula et al., 1976; Jolley et al., 1973). Gal_3 was prepared according to Aspinall et al. (1958). All experiments were performed in phosphate-buffered saline (PBS: 0.01 M sodium phosphate and 0.15 M sodium chloride, pH 7.4).

Kinetic measurements were done on a temperature jump spectrofluorometer (Rigler et al., 1974). Capacitor discharge of 20 kV raised the temperature of the solution by 5.2 °C from 20 ± 0.1 °C in ~1 μs. Protein solutions were excited at 280 nm; emitted light was collected through a WG 320 glass filter (cutoff 320 nm; Jena Glass Schott, Mainz, W. Germany). The averaged change in fluorescence from two photomultipliers was divided by the signal from a reference photomultiplier (X/Y mode) (Rigler et al., 1974) and fed into a Biomation 802 transient recorder (Biomation, Cupertino, CA) operating on two time bases, each employing 500 channels out of the total 1000. Time base durations were chosen in order to extract maximum information from the signal. Two different rise time filters were used, each less than 1% of its corresponding time base. At each concentration, the sum of at least five relaxation curves was recorded on magnetic tape using a recorder operated by a Hewlett-Packard 2100 minicomputer and then transferred to an IBM 370/165 computer for detailed analysis. The curves were fitted to a sum of exponents by using a modified Marquart algorithm (Fletcher, 1971). The quality of the fit was determined from the deviation between experimental data and the simulated curve, as well as by the autocorrelation function (Grinvald & Steinberg, 1974); Figure 1 shows a sample analysis. The relaxation amplitudes were normalized as described earlier (Lancet & Pecht, 1976; Vuk-Pavlović et al., 1978). The experimental concentration dependences of the relaxation times and amplitudes were fitted to expressions derived according to Castellan (1963) and Jovin (1975) for each specific reaction mechanism (see Results). Fitting was performed by minimizing the function

$$\sum_{i=1}^{N}\left[\left(\frac{CA_i - A_i}{A_i}\right)^2 + \left(\frac{1/C\tau_i - 1/\tau_i}{1/\tau_i}\right)^2\right] \qquad (1)$$

where CA_i and A_i are the calculated and experimental amplitudes at each reactant concentration, respectively, $C\tau_i$ and τ_i are the calculated and experimental relaxation times, respectively, and N is the number of different concentrations examined. The fitting was done by using a NAG library subroutine which allows placement of constraints on parameters and their functions (Gill & Murray, 1978). The most accurate points with large amplitude were given higher weight in the fitting. Application of this program yields a complete set of kinetic and thermodynamic parameters for a given reaction mechanism.

Fluorescence Titrations. Determination of the change in protein fluorescence upon Gal_3 binding was carried out by titration of the proteins with concentrated Gal_3 solution on a Perkin-Elmer MPF 44A spectrofluorometer in the ratio mode at 25 °C. The intrinsic fluorescence of the proteins (excitation at 280 nm and recorded emission from 320 to 350 nm) was measured at several hapten concentrations. Data were corrected for dilution, and the maximum fluorescence change upon binding was calculated.

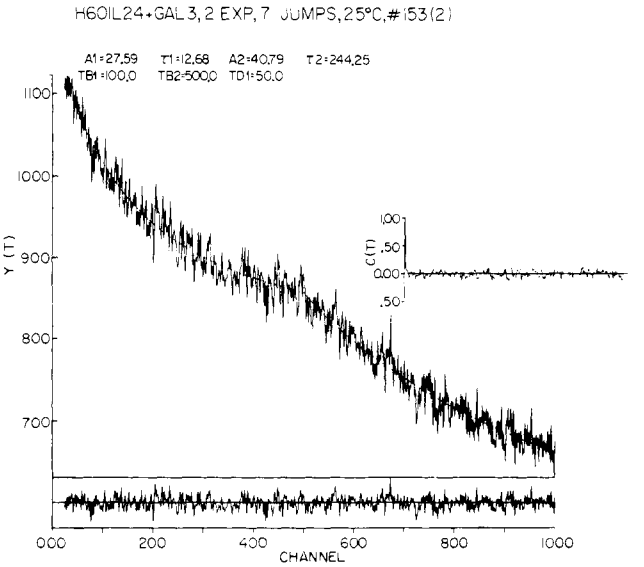

FIGURE 1: Example of the analysis and fitting of temperature jump–relaxation curves monitored via changes in emission. Protein $H^{601}L^{24}$ concentration was 8.84×10^{-7} M sites and Gal_3 concentration was 1.55×10^{-4} M. The presented data are a sum of seven temperature jumps. The ordinate shows digitized Biomation units, and the abscissa shows the channel number of the Biomation memory. In the first 50 ms (TD1) after the jump the sampling rate was 100 ms/1000 channels (TB1), and after 500 channels were recorded the time base was switched to 500 ms/1000 channels (TB2). At the same time the rise time filter of the amplifier was changed from 0.5 to 5 ms. The data are fitted to two exponents, and the resulting amplitudes (A1 and A2, in millivolts) and relaxation times (τ_1 and τ_2, in milliseconds) are presented. The solid line is drawn by using these parameters. The total signal after the jump was 8000 mV. The insert, top right, is the autocorrelation analysis of the fit. The lower part of the figure shows the deviation between experimental and fitted curves, normalized to the largest deviation. Additional details are under Materials and Methods.

Results

The relaxation spectra of all the protein–hapten equilibria studied, with the exception of $H^{539}L^{24}$, were found to fit a biexponential decay function. In the case of $H^{539}L^{24}$, the signal amplitude was insufficient for an accurate analysis, probably due to the unfavorable combination of a relatively small fluorescence enhancement ($\Delta F_{overall}$ = 12%) with a low enthalpy change. In all other antibody–hapten systems studies, the two relaxation times were observed over the whole range of hapten concentration examined and were resolved by at least a factor of 8. No relaxations were detected for any of the reactants alone.

The concentration dependences of the fast and slow reciprocal relaxation times ($1/\tau_f$ and $1/\tau_s$, respectively) and the corresponding amplitudes are shown in Figures 2–5. For all four proteins $1/\tau_f$ increased linearly, while $1/\tau_s$ leveled off with increasing hapten concentration. This is an indication that the fast relaxation results from a bimolecular association and the slower one results from a monomolecular step attributed here to protein isomerization. Three mechanisms, which may be considered for describing antibody–hapten interactions with the observed monomolecular slow step, have previously been discussed extensively (Vuk-Pavlović et al., 1978; Lancet & Pecht, 1976). The square mechanism is a thermodynamically

$$\begin{array}{ccc} H + T_0 & \underset{k_{-T}}{\overset{k_T}{\rightleftharpoons}} & T_1 \\ k_0 \downarrow\uparrow k_{-0} & & k_1 \downarrow\uparrow k_{-1} \\ H + R_0 & \underset{k_{-R}}{\overset{k_R}{\rightleftharpoons}} & R_1 \end{array} \qquad (2)$$

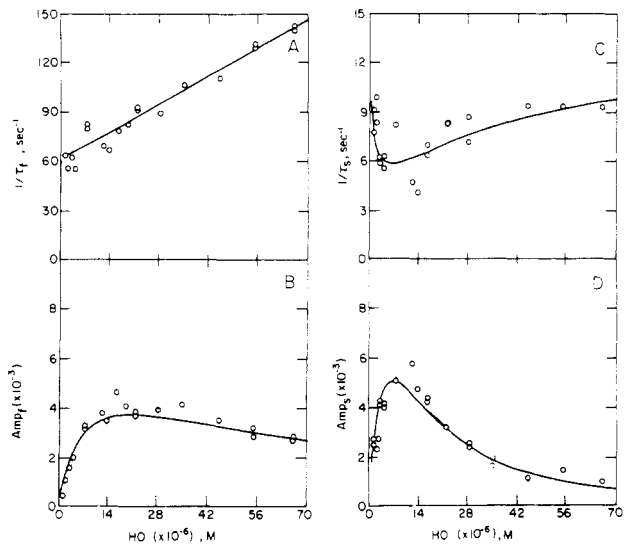

FIGURE 2: Dependence of fast (A and B) and slow (C and D) reciprocal relaxation times and amplitudes of T-601 on total Gal_3 concentration at 25 °C. Solid lines are drawn by using the best-fit parameters from Table I. Protein concentration is 1×10^{-6} M sites.

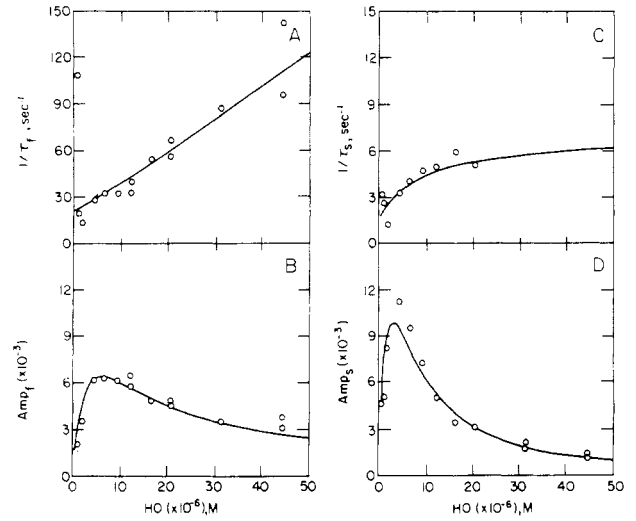

FIGURE 3: Dependence of fast (A and B) and slow (C and D) reciprocal relaxation times and amplitudes of $H^{24}L^{539}$ on total Gal_3 concentration at 25 °C. Protein concentration is 1×10^{-6} M sites.

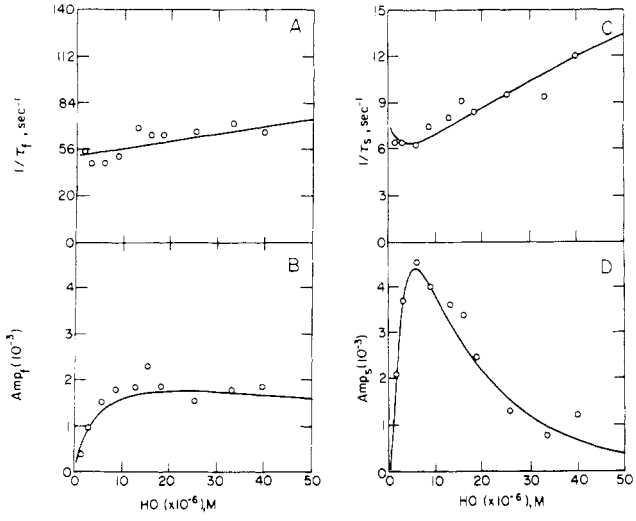

FIGURE 4: Dependence of fast (A and B) and slow (C and D) reciprocal relaxation times and amplitudes of $H^{24}L^{601}$ on total Gal_3 concentration at 25 °C. Protein concentration is 1.2×10^{-6} M sites.

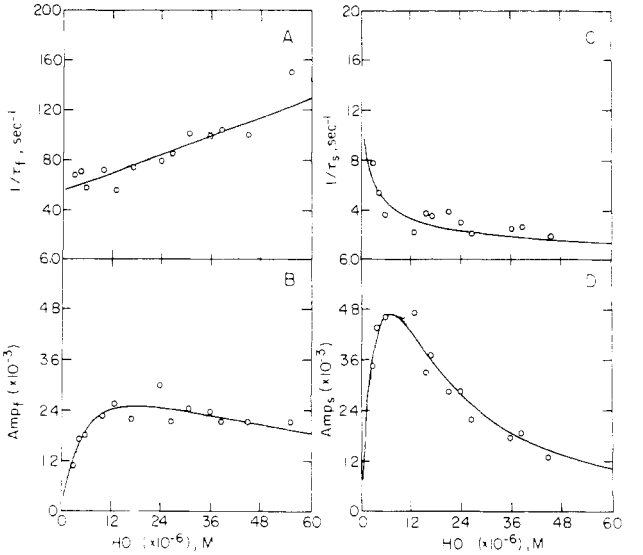

FIGURE 5: Dependence of fast (A and B) and slow (C and D) reciprocal relaxation times and amplitudes of $H^{601}L^{24}$ on total Gal_3 concentration at 25 °C. Protein concentration is 8.8×10^{-7} M sites.

general one and fully describes the kinetic and thermodynamic parameters of the reaction. Moreover, the binding behavior of one of the parent proteins studied earlier (X-24) (Vuk-Pavlović et al., 1978) was shown to fit only mechanism 2, thus making it the only basis for comparison of the systems. Therefore, we analyzed our data according to mechanism 2, where H denotes hapten, T_0 and R_0 represent the two free protein conformations, and T_1 and R_1 are the two conformations of the protein–hapten complexes (Monod et al., 1965). Three relaxation times are expected for this mechanism. In the case of the association steps being faster than the conformational transitions, two of the relaxation times represent the T and R associations and one represents the isomerization step (Castellan, 1963), each slower step being influenced by the faster. However, only two relaxation times were observed for all four protein–hapten systems studied. This was also the case for the previously studied X-24, J-539, and M-460 (Vuk-Pavlović et al., 1978; Lancet & Pecht, 1976). This behavior has been interpreted, as previously, by assuming that no spectral change occurs in one of the association steps. The concentration dependence of $1/\tau_f$ is used to resolve the question of whether the observed association should be assigned to the T or R state. Since the isomerization is kinetically and thermodynamically uncoupled from the faster association within the limits of time required for the latter to reach equilibrium and since the hapten concentration is essentially buffered for most of the range examined, we may approximate that $1/\tau_f = k_{on}H_0 + k_{off}$ (H_0 is total hapten concentration and k_{on} and k_{off} are the rate constants for the association and dissociation, respectively). The slope and intercept of the straight lines drawn through the points of part A of Figures 2–5 yield k_{on} and k_{off}. The equilibrium constant of this association step is $K_{ass} = k_{on}/k_{off}$. The square mechanism defines the relation between association constants as $K_T < K_{overall} < K_R$ (Lancet & Pecht, 1976). K_{ass} obtained from part A of Figures 2–5 in each case is smaller than $K_{overall}$ which was determined separately by static fluorescence titrations. Thus, it is concluded that the fast step represents the T association in all Ig–hapten systems studied. The zero fluorescence change must therefore be attributed to the R association step, $\Delta F_R = 0$. The concentration dependences were fitted to the following equations derived according to Castellan (1963) and

Table I: Kinetic and Thermodynamic Parameters for the Reaction of the Immunoglobulins with Gal_3 at 25 °C

	X-24[a]	J-539[a]	T-601	$H^{24}L^{539}$	$H^{24}L^{601}$	$H^{601}L^{24}$
K (M^{-1})	1.2×10^5	1.2×10^5	1.0×10^5	2.9×10^5	2.1×10^5	1.2×10^5
K_T (M^{-1})	4.5×10^4	5.0×10^4	2.0×10^4	1.0×10^5	9.0×10^3	2.3×10^4
K_R (M^{-1})	2.7×10^5	2.0×10^5	1.6×10^6	6.3×10^5	5.4×10^5	5.0×10^5
K_0	0.50	0.93	0.05	0.55	0.60	0.25
K_1	3.0	3.7	4.3	3.3	36.5	5.6
ΔH (kcal/mol)	−10.6	−11.3	−5.4	−10.2	−6.2	−5.1
ΔH_T (kcal/mol)	−10.6	−12.8	−6.2	−10.8	−14.6	−5.0
ΔH_R (kcal/mol)	−10.5	−10.6	−3.6	−9.8	−6.5	−5.5
ΔH_0 (kcal/mol)	0.01	−0.63	−1.75	−0.46	0.91	0.50
ΔH_1 (kcal/mol)	0.00	0.53	0.81	0.57	9.00	−0.04
ΔF	0.25	0.20	0.22	0.24	0.16	0.21
ΔF_T	0.31	0.20	0.26	0.25	0.25	0.26
ΔF_0	0.41	0.30	0.22	0.44	0.26	0.26
ΔF_1	0.10	0.009	−0.03	0.19	0.007	0.002
k_T (M^{-1} s^{-1})	4.5×10^5	1.2×10^6	1.2×10^6	2.1×10^6	4.7×10^5	1.2×10^6
k_{-T} (s^{-1})	10.0	24.8	60.9	20.0	52.0	54.7
k_0 (s^{-1})	1.05	1.77	0.78	0.50	2.90	2.36
k_{-0} (s^{-1})	2.09	1.91	14.20	0.91	4.90	9.37
k_1 (s^{-1})	0.30	5.72	11.40	5.36	33.30	0.06
k_{-1} (s^{-1})	0.10	1.56	2.65	1.64	0.91	0.01

[a] From Vuk-Pavlović et al. (1978). Enthalpy and fluorescence parameters for the binding of X-24 were obtained by us recently from the Data of Vuk-Pavlović et al. (1978) by using more powerful methods of analysis (see Materials and Methods). We estimated the error by simulations and parameter variation for most parameters as ±20%. For ΔH_0, ΔH_1, ΔF_0, and ΔF_1, the estimated error is ±50%.

Jovin (1975) which are identical with those employed in our previous work (Vuk-Pavlović et al., 1978):

$$1/\tau_f = k_T g_{11} T_0 H \quad (3)$$

$$1/\tau_s = |g_3|(k_1 T_1 + k_0 T_0)/|g_2| \quad (4)$$

$$A_f = \Delta H_T \Delta F_T \Delta T/(g_{11} A_0 R T^2) \quad (5)$$

$$A_s = |g_2|(Q_{13}\Delta F_T + Q_{23}\Delta F_R + \Delta F_0) \times (Q_{13}\Delta H_T + Q_{23}\Delta H_R + \Delta H_0)\Delta T/(|g_3| R T^2 A_0) \quad (6)$$

where ΔF_i and ΔH_i are the normalized fluorescence change and standard enthalpy change of step i, respectively, A_0 is the total protein concentration, and

$$Q_{13} = (g_{12}g_{23} - g_{13}g_{22})/|g_2|$$
$$Q_{23} = (g_{12}g_{13} - g_{11}g_{23})/|g_2|$$

g_{ij} and $|g_i|$ are an element and a principal partial determinant of the Castellan g matrix (Castellan, 1963):

$$g = \begin{vmatrix} \frac{1}{T_0} + \frac{1}{T_1} + \frac{1}{H} & \frac{1}{H} & \frac{1}{T_0} \\ \frac{1}{H} & \frac{1}{R_0} + \frac{1}{R_1} + \frac{1}{H} & -\frac{1}{R_0} \\ \frac{1}{T_0} & -\frac{1}{R_0} & \frac{1}{T_0} + \frac{1}{R_0} \end{vmatrix} \quad (7)$$

T_0, T_1, R_0, R_1, and H are the equilibrium concentrations of the respective species. Equations 3–7 were derived under the assumption that the T association is the fastest in the system. An attempt was also made to fit the data while assuming that the R association step is faster, with coupled T association; however, these conditions allowed no satisfactory fit. The assumption that $\Delta F_R = 0$ was also examined by trying to fit the data to a mechanism with the two association steps having close, unresolvable relaxation times. The observed fast relaxation in this case would be the weighted sum of the relaxations of two association steps (Schwarz, 1968). As a result, we obtained very small ΔF_R values (0.01–0.02), which are within the error limits of $\Delta F_R = 0$ and thus justified our assumption. ΔH_R values, however, were significant, thus ruling out the assumption of $\Delta H_R = 0$ as an explanation for the absence of a third relaxation. The best-fit parameters obtained as a result of the analysis are presented in Table I. ΔH_0 and ΔF_0 values different from zero (Table I) imply that there is a small amplitude relaxation in the free protein. We were looking for such a relaxation (especially in the case of T-601, which has a higher ΔH_0) but were unable to detect it, probably due to the low signal to noise ratio. The $K_{overall}$ values are in reasonably good agreement with those obtained by fluorescence titrations (Manjula et al., 1976). The following functional and boundary constraints were imposed during the fitting procedure: (1) the equilibrium and rate constants were kept positive; (2) $K_R > K_T$ as required by the employed mechanism; (3) $K_{overall}$ and $\Delta F_{overall}$ were kept equal to the values obtained by independent static fluorescence titrations; (4) $0 < -\Delta H_{overall} < 25$ kcal/mol as one expects from the thermodynamics of hapten binding.

Discussion

The results from detailed analysis of the kinetic data (Table I) show the thermodynamic and kinetic behavior of both the parent and hybrid immunoglobulins to be consistent with the square model (eq 2), in which the protein exists in two conformational states, T and R, each differing in its affinity toward hapten, i.e., $K_R > K_T$ (Lancet & Pecht, 1976; Monod et al., 1965). The overall association constants of the hybrids were previously shown to be similar to those of their respective constitutent parent molecules (Manjula et al., 1976). Our present data further demonstrate that the binding constants of each conformer, K_T and K_R, are similar to those of their respective parent proteins. This holds also for the specific association and dissociation rate constants, k_T and k_{-T} (Table I). The association rates are similar to those found for other saccharide-binding antibodies (Maeda et al., 1977; Pecht, 1976) and are 2 orders of magnitude slower than the association rates observed for nitroaromatic-binding immunoglobulins (Pecht & Lancet, 1977). Even slower rates were found for the binding of saccharides by lectins (Clegg et al., 1977; Loontiens et al., 1977). As suggested earlier (Pecht & Lancet, 1977; Vuk-Pavlović et al., 1978), these slower rates of saccharide-binding proteins may be caused by the ligand's high flexibility and/or by the need to disrupt and form several hydrogen bonds upon association. All the hybrids, like their parent proteins, show small positive free energy changes upon conformational transition of the free protein, ΔG_0. This implies

that the T_0 conformer is more stable, although the difference in free energy between the two states is relatively small. Conversely, the free energy change of the conformational transition of the bound protein is in all cases negative. The equilibrium between T and R states is therefore shifted upon binding and R_1 becomes the predominant conformation. These results constitute a further illustration of hapten-induced conformational change in immunoglobulins and suggest their general prevalence.

A wide range of experimental approaches has shown that conformational changes are induced in immunoglobulins upon hapten or antigen binding [for a review, see Metzger (1978)]. Among them are ESR of spin-labels (Käiväräinen & Nezlin, 1976), thermal perturbation spectroscopy (Zav'yalov et al., 1977), ^{35}Cl NMR (Vuk-Pavlović et al., 1979), circular polarization of fluorescence (Schlessinger et al., 1975; Jaton et al., 1975), and CD (Holowka et al., 1972). Some of these studies indicated that the conformational transition extends beyond the combining site (Zav'yalov et al., 1977; Schlessinger et al., 1975). A clear illustration of longitudinal interaction between variable and constant immunoglobulin domains has recently been made by the kinetic study of the binding of variable and constant domains of a light chain to Fd, the first two domains of a heavy chain (Klein et al., 1979). It was found that the binding of the C_L domain occurs much faster when V_L is already bound to Fd. Our recent studies of the light-chain dimer of protein 315 (Lancet et al., 1977; Zidovetzki et al., 1979) have demonstrated the profound influence of the intact interchain disulfide bond at the C terminus on the hapten binding properties of the dimer binding site at the N terminus. Previously it was noted (Vuk-Pavlović et al., 1978) that in X-24 and J-539 the transition probably involves a large portion of the Fab. As these hybrids behave in a kinetically similar manner to their parent proteins and in view of the above-mentioned observations, it is assumed that this conclusion can also be applied to the recombinants.

Changes in the amino acid sequence, which in the presently investigated systems occur in the complementarity-determining regions (CDR's) as well as in the frameworks (FR's) of the heavy chains (Rao et al., 1979), apparently do not change the inter- or intrachain modes of domain interaction. This implies that the conformational transition is determined by the overall tertiary structure and possibly is implemented as a shift in the relative positions of the heavy and light chains.

An illustration of the Tg domains as structural units can be found in the X-ray crystallographic study of the Mcg light-chain dimer (Schiffer et al., 1973). This dimer's folding parallels that of Fab, with one of the light chains adapting the conformation which resembles that of the Fab heavy chain. This is obtained by structural changes in the light chain's "switch" region, primarily between domains.

An attempt has been made here to correlate the binding and isomerization parameters of each hybrid with those of its parent proteins, in order to determine whether one of the chains dominates the hybrid's behavior. A correlation was found only for the two isomerization rates of the bound hybrids (k_1 and k_{-1}), which are significantly closer to those values of the parent light-chain donor (Table I). This result is somewhat unexpected; though the light chain of J-539 differs from those of T-601 and X-24 at five and six positions, respectively, light chains of T-601 and X-24 are identical at all but one position, no. 100 (S. Rudikoff, D. N. Rao, C. P. J. Glaudemans, and M. Potter, unpublished experiments). The sensitivity of the kinetic parameters of this step causing their variation over several orders of magnitude is noteworthy. The heavy chains of these proteins, on the other hand, have 7–14 substitutions, both in CDR's and FR's, including residues that contact the V_L domain (Rao et al., 1979).

Similarities in the basic tertiary structures of any given domains, as determined by X-ray crystallography, are revealed in the unchanged mode of interaction between heterologous chains of a recombinant Ig. Such evidence supports the proposed mechanism for generation of new antibodies with different specificities by pairing different light chains with the same heavy chain and vice versa (Kabat, 1976; Nisonoff et al., 1975). Furthermore, this work provides new evidence for the generality of hapten-induced conformational changes.

Acknowledgments

We thank Mark Holms for his help in preparation of the manuscript.

References

Aspinall, G. O., Auret, B. J., & Hirst, E. L. (1958) *J. Chem. Soc.*, 4408.

Castellan, G. W. (1963) *Ber. Bunsenges. Phys. Chem. 67*, 898.

Clegg, R. M., Loontiens, F. G., & Jovin, T. M. (1977) *Biochemistry 16*, 167.

Fletcher, R. (1971) in Harwell Subroutine Library, Atomic Energy Research Establishment, Harwell, U.K. (Subroutine VB01A).

Gill, D. E., & Murray, W. (1978) in NAG Fortran Library from the Numerical Algorithms Group at Oxford University, Mark 6 (Subroutine E04UAF).

Grinvald, A., & Steinberg, I. Z. (1974) *Anal. Biochem. 59*, 583.

Holowka, D. A., Strosberg, A. D., Kimball, J. W., Haber, E., & Cathou, R. E. (1972) *Proc. Natl. Acad. Sci. U.S.A. 69*, 3399.

Jaton, J.-C., Huser, H., Braun, D. G., Givol, D., Pecht, I., & Schlessinger, J. (1975) *Biochemistry 14*, 5312.

Jolley, M. E., Rudikoff, S., Potter, M., & Glaudemans, C. P. J. (1973) *Biochemistry 12*, 3039.

Jovin, T. M. (1975) in *Biochemical Fluorescence Concepts* (Chen, R. F., & Edelhoch, H., Eds.) Vol. 1, p 305, Marcel Dekker, New York.

Kabat, E. A. (1976) *Structural Concepts in Immunology and Immunochemistry*, Holt, Rinehart and Winston, New York.

Käiväräinen, A. I., & Nezlin, R. S. (1976) *Biochem. Biophys. Res. Commun. 68*, 270.

Klein, M., Kortan, C., Kells, D. I. C., & Dorrington, K. J. (1979) *Biochemistry 18*, 1473.

Lancet, D., & Pecht, I. (1976) *Proc. Natl. Acad. Sci. U.S.A. 73*, 3549.

Lancet, D., Licht, A., Schechter, I., & Pecht, I. (1977) *Nature (London) 269*, 827.

Loontiens, F. G., Glegg, R. M., Van Landschoot, A., & Jovin, T. M. (1977) *Eur. J. Biochem. 78*, 465.

Maeda, H., Schmidt-Kessen, A., Engel, J., & Jaton, J.-C. (1977) *Biochemistry 16*, 4086.

Manjula, B. N., Glaudemans, C. P. J., Mushinski, E. B., & Potter, M. (1976) *Proc. Natl. Acad. Sci. U.S.A. 73*, 932.

Manjula, B. N., Mushinski, E. B., & Glaudemans, C. P. J. (1977) *J. Immunol. 119*, 867.

Metzger, H. (1978) *Contemp. Top. Mol. Immunol. 7*, 119.

Monod, J., Wyman, J., & Changeux, J. T. (1965) *J. Mol. Biol. 12*, 88.

Nisonoff, A., Hopper, J. E., & Spring, S. B. (1975) *The Antibody Molecule*, p 224, Academic Press, New York and London.

Padlan, E. A. (1977) *Q. Rev. Biophys. 10*, 35.

Pecht, I. (1976) in *The Immune System* (Melchers, F., & Rajewsy, K., Eds.) 27 Mosbacher Colloquium, p 41, Springer-Verlag, Berlin and Heidelberg.
Pecht, I., & Lancet, D. (1977) in *Chemical Relaxation in Molecular Biology* (Pecht, I., & Rigler, R., Eds.) p 306, Springer-Verlag, Berlin and Heidelberg.
Poljak, R. J. (1975) *Nature (London) 256*, 373.
Poljak, R. J., Amzel, L. M., & Phizackerley, R. P. (1976) *Prog. Biophys. Mol. Biol. 31*, 67.
Rao, D. N., Rudikoff, S., Krutzsch, H., & Potter, M. (1979) *Proc. Natl. Acad. Sci. U.S.A. 76*, 2890.
Rigler, R., Rabl, C. R., & Jovin, T. M. (1974) *Rev. Sci. Instrum. 45*, 580.
Schiffer, M., Girling, R. L., Ely, K. R., & Edmundson, A. B. (1973) *Biochemistry 12*, 4620.
Schlessinger, J., Steinberg, I. Z., Givol, D., Hochman, J., & Pecht, I. (1975) *Proc. Natl. Acad. Sci. U.S.A. 72*, 2775.
Schwarz, G. (1968) *Rev. Mod. Phys. 40*, 206.
Vuk-Pavlović, S., Blatt, Y., Glaudemans, C. P. J., Lancet, D., & Pecht, I. (1978) *Biophys. J. 24*, 161.
Vuk-Pavlović, S., Isenman, D. E., Elgavish, G. A., Gafni, A., Licht, A., & Pecht, I. (1979) *Biochemistry 18*, 1125.
Zav'yalov, V. P., Abramov, V. M., Skortzov, V. G., & Troitsky, G. V. (1977) *Biochim. Biophys. Acta 493*, 359.
Zidovetzki, R., Licht, A., & Pecht, I. (1979) *Proc. Natl. Acad. Sci. U.S.A. 76*, 5848.

Carbon-13 Nuclear Magnetic Resonance Studies and Anomeric Composition of Ketohexose Phosphates in Solution†

Theodore A. W. Koerner, Jr.,‡ Ronald J. Voll, Lewis W. Cary,§ and Ezzat S. Younathan*

ABSTRACT: The Fourier transform ^{13}C NMR spectra of the following ketohexose phosphates were studied: D-fructose 6-phosphate (**1**), D-fructose 1-phosphate (**2**), D-fructose 1,6-bisphosphate (**3**), D-psicose 6-phosphate (**4**), D-tagatose 6-phosphate (**5**), and L-sorbose 6-phosphate (**6**). All ^{13}C resonances were assigned through the use of off-resonance decoupling studies, ^{31}P–^{13}C couplings, and chemical shift comparisons with 2,5-anhydro-D-hexitol phosphates (**7**–**10**). Integration of the signal intensities of the C-2 carbons yielded the following equilibrium percentage compositions for α (**a**) and β (**b**) furanose anomers (±2%): (at 16.5 °C) **1a** 19, **1b** 81, **4a** 76, **4b** 24, **5a** 17, **5b** 83, **6a** 82, **6b** 18; (at 35 °C) **2a** 24, **2b** 76, **3a** 23, **3b** 77. These values can be quantitatively predicted through conformational analysis of the furanose ring of the sugars if it is assumed that (1) ketofuranose 6-phosphates exist in the $^4T_3$, $^OT_2$, and $^OT_5$ twist conformations (or mirror-image conformations for L forms) and (2) a proposed set of twist conformation interaction energies is operative. Due to the presence of the C-2 hydroxymethyl group, a new anomeric interaction ($\Delta 3$ effect) must be proposed for the ketofuranoses that is analogous to Reeves's $\Delta 2$ effect for aldopyranoses. This conformational analysis yields concentrations for the $^4T_3$ conformation of β-D anomers, or the $^3T_4$ conformation of α-L anomers, of ketofuranose 6-phosphates that vary directly with the substrate activity of each sugar for phosphofructokinase (EC 2.7.1.11). This correlation suggests that this enzyme prefers these conformations for the furanose rings of its substrates. The values for $^3J_{POCC}$ allow the rotameric compositions of the phosphate groups of **1**–**10** to be calculated. In all cases, the trans-periplanar rotamer predominates (38–63%).

Ketohexose phosphates play important roles as intermediates and regulators of carbohydrate metabolism. In fact, the isolation of fructose 1,6-bisphosphate (fructose-1,6-P_2)[1] from yeast in 1906 provided the very basis for the modern concept of metabolic "intermediate" (Korman, 1974). Fructose-1,6-P_2 is now known to play a central role in glucose metabolism and to affect the rate of a large variety of physiologically important enzyme reactions (Kirtley & McKay, 1977). Fructose-6-P is the only intermediate common to the glycolytic, gluconeogenic, pentose, and amino sugar pathways. Tagatose phosphates may be important intermediates in galactose metabolism (Bissett & Anderson, 1973; Koerner et al., 1976). The 6-phosphates of fructose, psicose, tagatose, and L-sorbose have all been shown to be substrates of the regulatory enzyme phosphofructokinase (Koerner et al., 1976). The 1,6-bisphosphates of L-sorbose and tagatose as well as fructose are substrates for aldolase (Tung et al., 1954).

An often overlooked aspect of the biochemistry of ketohexose phosphates is that these sugars in solution are mixtures of several constitutional and configurational isomers (tautomers and anomers), each present in different concentrations and capable of displaying different affinities and reactivities (anomeric specificity) for enzyme catalytic and allosteric sites

† From the Department of Biochemistry, Louisiana State University, Baton Rouge, Louisiana 70803. *Received October 11, 1979.* This work was supported by Grant No. AM-21307 from the National Institutes of Health and Grant No. PGM 77-27286 from the National Science Foundation. A preliminary account of this work was presented, in part, at the XIth International Congress of Biochemistry held in Toronto, Canada, July 8–13, 1979. This paper is dedicated to Dr. Richard E. Reeves, whose meritorious contributions to our understanding of the chemistry and metabolism of carbohydrates have been an inspiration to us and to many workers in this field for several decades.

‡ Present address: Department of Laboratory Medicine, Yale University School of Medicine, New Haven, CT 06510.
§ Present address: Nicolet Technology Corp., Mt. View, CA 94041.

[1] Abbreviations used: P or PO_3^{2-}, phosphate group; P_2, bisphosphate; δ, chemical shift; $\Delta\delta$, chemical shift difference; $\Delta\Delta\delta$, difference in chemical shift differences; ppm, parts per million; J, coupling constant; FT, Fourier transform; α-1, α-furanose C-1, etc.; β-1, β-furanose C-1, etc.; E and T, envelope and twist conformations of the furanose ring. All sugars are D unless labeled L.

0006-2960/80/0419-2795$01.00/0